Application of the TRANSURANUS code for the fuel pin design process of the ALFRED reactor

Lelio Luzzi [a,*], Antonio Cammi [a], Valentino Di Marcello [b,1], Stefano Lorenzi [a], Davide Pizzocri [a], Paul Van Uffelen [b]

[a] *Politecnico di Milano – Department of Energy, Enrico Fermi Center for Nuclear Studies (CeSNEF), via Ponzio 34/3, 20133 Milano, Italy*
[b] *European Commission, Joint Research Centre, Institute for Transuranium Elements, PO Box 2340, 76125 Karlsruhe, Germany*

Article history:
Received 16 November 2013
Received in revised form 6 June 2014
Accepted 22 June 2014

1. Introduction

The Lead-cooled Fast Reactor (LFR) has been selected by the Generation IV International Forum as one of the candidates for the next generation of nuclear power plants (GIF, 2002). Advanced reactor concepts cooled by Heavy Liquid Metals (HLM) ensure a great potential for plant simplifications and higher operating efficiencies compared to other coolants, nevertheless introducing additional safety concerns and design challenges (Cacuci, 2010). Reactor conditions of HLM-cooled reactor designs (e.g., extended exposure to neutron irradiation, high temperature, corrosive environment) impose challenges for engineers and designers concerning the selection of structural and cladding materials. Key guidance on material behaviour and help to improve the design can be achieved by means of fuel pin performance codes.

In this paper, the fuel pin performance analysis is aimed at optimizing the conceptual fuel pin design of the Advanced Lead-cooled Fast Reactor European Demonstrator (ALFRED). ALFRED is a pool-type, small power reactor (Alemberti et al., 2010)

* Corresponding author. Tel.: +39 02 2399 6326; fax: +39 02 2399 6309.
E-mail address: lelio.luzzi@polimi.it (L. Luzzi).
[1] Current address: Karlsruhe Institute of Technology, Institute for Neutron Physics and Reactor Technology (INR), Hermann-von-Helmholtz Platz 1, D-76344 Eggenstein-Leopoldshafen, Germany.

Table 1
ALFRED reactor specifications.

Reactor specification	
Thermal power [MW]	300
Fuel residence time [y]	5
Coolant inlet temperature [°C]	400
Average coolant outlet temperature [°C]	480
Coolant mass flow rate [kg s^{-1}]	≈25,700
Average coolant velocity [m s^{-1}]	≈1.4

conceived to be fully representative of the industrial scale reference system proposed within the LEADER (Lead Cooled European Advanced Demonstration Reactor) EURATOM Project (http://www.leader-fp7.eu). Since the fuel pin behaviour is determined by the synergy of several phenomena (heat transfer to the coolant, creep, swelling and corrosion of the cladding, relocation, densification, creep, and swelling of the fuel, fission gas release, etc.), a fuel pin analysis can be adequately accomplished by means of integral performance codes. In the present work, the TRANSURANUS code (Lassmann, 1992; Di Marcello et al., 2013) developed at JRC-ITU (Karlsruhe) has been extended and adopted for the simulation of the ALFRED reactor core operational conditions.

The austenitic steel Ti-15-15 is considered to be the cladding material in the ALFRED reactor, as well as for other fast reactor systems like the Accelerator-Driven System MYRRHA (Aït Abderrahim et al., 2012) and the Sodium Fast Reactor ASTRID (Gavoille et al., 2013). Despite the lower resistance to void swelling compared to the ferritic-martenstic steel T91 (the former candidate material for the cladding), the austenitic steel has been selected due to the better thermal creep resistance, the good mechanical strength and because it has been already qualified and licensed in fast reactors.

In this paper, the fuel and cladding performance analysis aims at critically analysing the conceptual design of the fuel pin in order to improve the *safety-by-design* characteristics of the advanced generation of LFR systems. After the updating and refinement of the TRANSURANUS code material properties and models for the simulation of the Ti-15-15 cladding material in LFRs, the following strategy has been adopted consisting of four phases. First of all, a *reference case* for the ALFRED reactor fuel pin (phase 1) is defined with the selection of an Average Channel (AC) and Hot Channel (HC) case, representing the average and the hottest reactor conditions, respectively. The reference case has been selected adopting a "best estimate" approach for the fuel and cladding performance, namely the models and parameters with a high degree of confidence and reliability with respect to the experimental data are adopted. Secondly, a *sensitivity analysis* (phase 2) is carried out in order to investigate the modelling uncertainty, mainly due to lack or disagreement in experimental data. In particular, the sensitivity analysis has to focus on the models which have the largest impact on the main issues pointed out by the reference case analysis (e.g., if the reference case is characterized by large stress in the cladding, the models governing the gap size dynamics will be selected since they are the most relevant for this phenomenon). Based on the results of the sensitivity, a "*worst case" scenario* (phase 3) is identified. This case represents the "conservative" analysis of the fuel and cladding performance of the hot channel since the model options, which are more detrimental for cladding integrity, are applied. Finally, the TRANSURANUS code is adopted to provide *preliminary feedback* on the conceptual design (phase 4) according to indicative design limits. Based on the "worst case" scenario of the hot channel, simulations are performed with different values of tuneable design parameters (e.g., gap size or internal pin pre-pressurization) in order to improve the fuel and cladding performance behaviour of the ALFRED reactor. This process can be iterated according to designers feedback until the best solution is found.

Table 2
ALFRED fuel pin parameters.

Fuel pin design parameter	
Fuel type	MOX
Enrichment as Pu/(Pu + U) [wt.%] (inner zone)	21.7
Enrichment as Pu/(Pu + U) [wt.%] (outer zone)	27.80
Fuel density [%] of theoretical density	95
O/M	1.97
Cladding	Ti-15-15
Fill gas	He
Pre pressurization [MPa]	0.1
Upper plenum volume [mm^3]	≈30,000
Upper plenum length [mm]	120
Active length [mm]	600
Lower plenum length [mm]	550
Cladding outer diameter [mm]	10.5
Cladding inner diameter [mm]	9.3
Fuel pellet outer diameter [mm]	9
Fuel pellet inner diameter [mm]	2
Pin pitch [mm]	13.86

Table 3
Isotopic specification for U and Pu (Sobolev et al., 2009).

Plutonium		Uranium	
Isotope	Fraction (wt.%)	Isotope	Fraction (wt.%)
^{238}Pu	2.332	^{234}U	0.003
^{239}Pu	56.873	^{235}U	0.404
^{240}Pu	26.997	^{236}U	0.010
^{241}Pu	6.105	^{238}U	99.583
^{242}Pu	7.693		

The paper is organized as follows. In Section 2, a brief introduction to the ALFRED reactor is provided along with the main features and design limits. In Section 3, after a short introduction of the TRANSURANUS code, the cladding and coolant modelling is described. In Section 4, the reference case of the ALFRED fuel pin is presented. In Section 5, the sensitivity analysis and the identification of the worst case scenario are discussed. Therefore, in Section 6, the optimization phase is reported. The main conclusions are drawn in Section 7.

2. Reactor description

ALFRED is a small-size (300 MW$_{th}$) pool-type LFR. The current primary system configuration (Alemberti et al., 2013) is depicted in Fig. 1. The reactor core is composed of wrapped hexagonal Fuel Assemblies (FAs), each one containing 127 fuel pins arranged in a triangular lattice. The 171 FAs are subdivided into two radial zones (57 inner and 114 outer) with different plutonium enrichments, and surrounded by two rows of dummy elements serving as reflector. In particular, the fuel considered for ALFRED consists of annular U–Pu Mixed OXide (MOX) pellets. As far as the cladding is concerned, the well-known Ti-15-15 steel has been selected because it was already qualified and licensed in fast reactors (Phenix, Superphenix). A 5-batches cycle without reshuffling with a 5 years fuel residence time is expected, i.e., 365 Equivalent Full Power Days (EFPD) per cycle leading to a total of 1825 EFPDs. The refuelling time between two cycles is foreseen to last about 15 days (Grasso et al., 2013). In Tables 1 and 2, the main specifications of the ALFRED reactor and fuel pin parameters are presented, respectively.

The fuel is composed of MOX pellets with 95% theoretical density and an Oxygen-to-Metal ratio (O/M) of 1.97. The fuel isotopic composition refers to a typical reactor grade Pu from the reprocessing of Pressurized Water Reactor (PWR) spent fuel (4.5% initial enrichment in ^{235}U, 45 MWd t^{-1} of burn-up, 15 years of cooling and storage) – see Table 3.

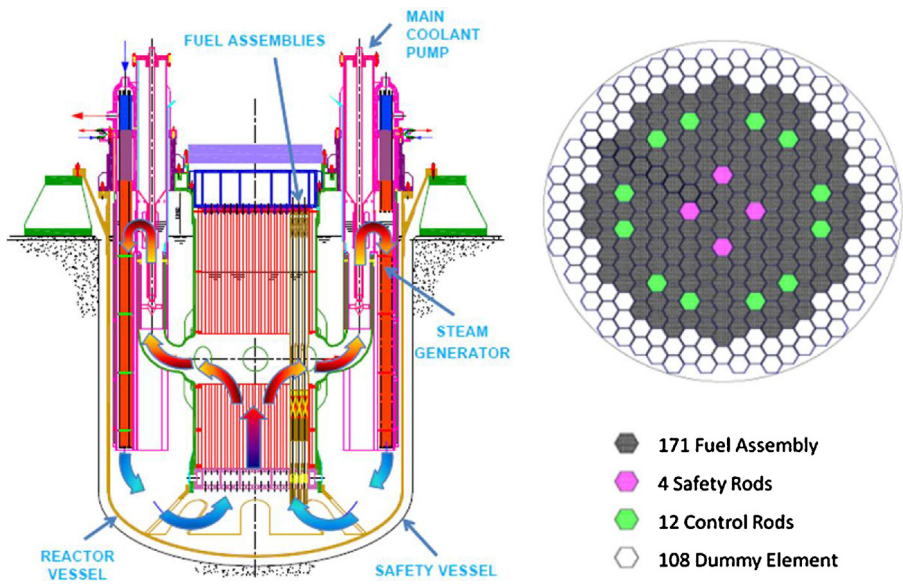

Fig. 1. ALFRED primary system and core layout.

Table 4
Indicative design limits for ALFRED reactor.

Quantity	Design indications	Reference
Peak fuel temperature	<2000 °C	Grasso et al. (2013)
Peak cladding temperature	<550 °C	Grasso et al. (2013)
Plenum pressure	<5 MPa	Grasso et al. (2013)
Maximum coolant velocity	<2 m s^{-1}	Alemberti et al. (2011)
Cladding $\Delta D/D$	<3%	IAEA (2012b)
Thermal creep strain (Option 1)	<0.2%	IAEA (2012b)
Thermal creep strain (Option 2)	<1%	NEA (2005)
Total creep strain	<3%	NEA (2005)
Cumulative damage function[a]	<0.2/0.3	IAEA (2012b)
Swelling strain	<5%	NEA (2005)
Instantaneous plastic strain	<0.5%	Vettraino and Luzzi (2001)

[a] The Cumulative Damage Function (CDF) is a pin lifetime parameter that considers the linear accumulation of the fraction damage calculated as ratio between the short time interval Δt and the time-to-rupture t_r. Fuel Adjacency Effect (FAE) is not taken into account in the evaluation of this parameter (Waltar et al., 2011).

2.1. Design limits

Indicative design limits have been collected from the open literature about the ALFRED design specific conditions (Grasso et al., 2013) and about liquid metal fast reactors in general (Vettraino and Luzzi, 2001; NEA, 2005; IAEA, 2012b). The design limits, presented in Table 4, involve the fuel and the cladding temperature, the plenum pressure, and the maximum plastic, creep and swelling strains. In particular, the most demanding issue regards the corrosion and the erosion problem of the lead environment (IAEA, 2012a). In this paper, the most conservative limits for the ALFRED fuel pin analyses are taken as reference in view of safety.

In order to prevent coolant-side aggression due to the high corrosive behaviour of lead, limits on cladding temperature and lead velocity are established and a coating on the external side is foreseen. Among the proposed solutions, the most promising candidate materials for the coating are the FeCrAlY alloy, realized through the so-called GESA (Gepulste ElektronenStrahlAnlage) treatment (Weisenburger et al., 2011), and the Al_2O_3 coating realized through Pulse Laser Deposition (PLD) (García Ferré et al., 2013).

3. Modelling

The integral fuel pin performance code TRANSURANUS (Lassmann, 1992; Di Marcello et al., 2013) has been adopted for the simulation of the ALFRED reactor core conditions. The code performs the thermal and mechanical analysis of a single fuel pin in the so-called 1.5 dimensional structure, and features a large flexibility that easily allows the implementation of new models and code modifications. Several strain components (elastic, plastic, creep and thermal strains, as well as strains due to cladding swelling and to fuel cracking, relocation, densification and swelling) can be processed, and the code can be applied both for steady state and transient analyses. TRANSURANUS has different models to describe the interacting phenomena affecting the fuel pin performance and the materials behaviour: nuclide analysis (Lassmann et al., 1994; Schubert et al., 2008); fission gas release (Lassmann and Benk, 2000); fuel relocation (Preusser and Lassmann, 1983); fuel restructuring and central void formation (Lassmann, 1992); oxygen redistribution (Lassmann, 1987); helium release (Di Marcello et al., 2013); gap conductance (Lassmann and Hohlefeld, 1987); fuel creep and swelling (Pesl et al., 1987).

Although TRANSURANUS has been extensively validated and assessed for Light Water Reactor (LWR) performance (Van Uffelen et al., 2007; TRANSURANUS Handbook, 2013), ITU has launched a research programme aimed at extending the TRANSURANUS capabilities for the simulation of fast reactor fuel pins in collaboration with many partners in the EU. In this work, thanks to a collaboration between Politecnico di Milano and ITU, the code has been further updated and improved concerning models and material properties for the cladding material Ti-15-15, in order to simulate the ALFRED reactor conditions. A brief summary of the main modifications for fast reactor environment concerning cladding and coolant is reported in the following sub-sections, whereas those for fuel have been published elsewhere (Di Marcello et al., 2012, 2013, 2014; Bouineau et al., 2013).

3.1. Cladding

The cladding material proposed for the ALFRED reactor is the austenitic stainless steel Ti-15-15. This class of steels has been

Table 5
AIM1 steel composition (Gavoille et al., 2013).

Steel	Cr [wt.%]	Ni [wt.%]	Mo [wt.%]	Mn [wt.%]	Si [wt.%]	Ti [wt.%]	C [wt.%]	B [ppm]
AIM1	15.0	15.0	1.50	1.5	0.90	0.4	0.09	60

adopted as cladding material in fast reactors in the early phase of the development of this technology (Waltar et al., 2011). After several years of reactor management (Superphenix) and irradiation campaigns (EBRII; Phenix), austenitic chromium-nickel (Cr-Ni) stainless steels have proven the best performance in reactor, showing excellent creep and good swelling resistance (Frost, 1994). In order to reduce the high swelling propensity caused by irradiation, several titanium-stabilized steels has been proposed (D9, 1.4970, etc.) exploiting the capability of TiC precipitates to increase the swelling incubation time. Moreover, the presence of silicon and boron can change the swelling and the creep features, respectively. Indeed, the concentration of each alloyed element has a paramount effect on the creep, on the swelling behaviour and on the rupture strain (Frost, 1994). Therefore, the composition can be adjusted to obtain best performance. Due to this strong dependence on the chemical composition, the Ti-15-15 represents actually a family of steels, and thus it does not correspond to a specific steel with a well-defined composition. This makes the modelling of the material behaviour, which has to be given via specific materials property correlations in TRANSURANUS more difficult. In this work, the reference steel is the Austenitic Improved Material (AIM1) developed at the CEA (cf. Table 5).

The foreseen cladding coating is modelled in the TRANSURANUS code by considering an additional thermal resistance (40 μm thickness) with a thermal conductivity of 15 W m^{-1} K^{-1} (Agosti et al., 2011). Therefore, mechanical analysis and irradiation effects have been disregarded in the present work for the coating.

Along with the correlations for the main thermal and mechanical properties (i.e., melting temperature, thermal expansion, density, specific heat, thermal conductivity, Young's modulus, Poisson ratio, yield and rupture strength, rupture strain) reported in Table 6, the main efforts are focused on swelling and creep, which are essential for the modelling of Ti-15-15 cladding.

3.1.1. Swelling

The void swelling is one of the major life limiting factors of cladding steels in fast reactors. This quantity, defined as the volume increase over the initial volume, is mainly influenced by the neutron fluence, and the temperature. Swelling is usually modelled (e.g., Waltar et al., 2011) considering an incubation period (at low displacements per atom – dpa) where no swelling occurs. Afterwards, the swelling starts increasing exponentially or linearly with the neutron fluence. According to several test experiments (Hübner, 2000; Bergmann et al., 2003), the swelling rate of Ti-15-15 is also affected by creep and applied stress, but due to the complexity of the phenomenon itself and to the lack of exhaustive information on the subject, both the effects are disregarded in the present work.

Since there are no suitable swelling models for Ti-15-15 in the open literature, a data-driven approach has been pursued, consisting in the derivation of a correlation based on experimental data available for this kind of steel (Hübner, 2000; Bergmann et al., 2003; Cheon et al., 2009; Dubuisson, 2013). In particular, two correlations have been implemented in the TRANSURANUS code (Fig. 2), since the lack of data and the uncertainties related to the different steel composition would preclude the development of a single equation able to reproduce all the experimental data. In this way, the above mentioned uncertainties can be assessed to some extent as will be shown by means of the sensitivity analysis (Section 5).

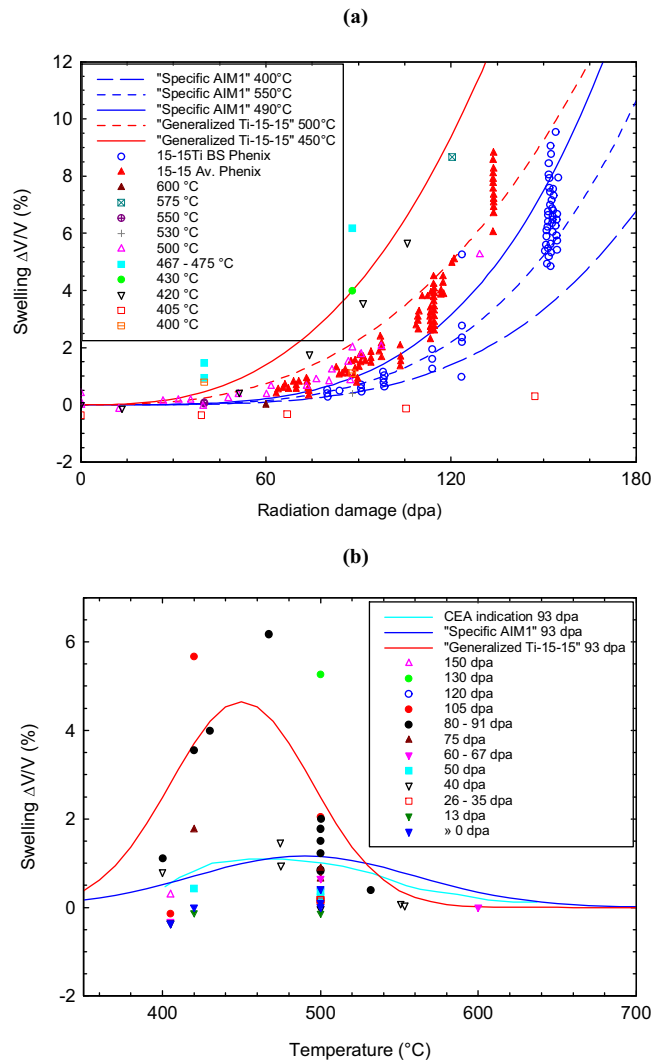

Fig. 2. "Specific AIM1" and "Generalized Ti-15-15" correlations against swelling experimental data (Bergmann et al., 2003; Cheon et al., 2009; Dubuisson, 2013; Hübner, 2000): (a) swelling deformation vs. dpa, (b) swelling deformation vs. temperature.

The "Generalized Ti-15-15" approach, adopted in Eq. (1), refers to a non-optimized version of the steel and it is aimed at representing the highest swelling values, occurring at 450 °C. The temperature dependence of the clad volume variation ($\Delta V/V$) is Gaussian-like, whereas the neutron fluence[1] follows a power-law function.

$$\frac{\Delta V}{V}[\%] = 1.5 \times 10^{-3} \exp\left[-2.5\left(\frac{T[^\circ\mathrm{C}] - 450}{100}\right)^2\right] \Phi^{2.75} \qquad (1)$$

[1] In Eqs. (1) and (2), Φ is the neutron fluence divided by 10^{22} n cm^{-2}.

Table 6
Correlations used in the cladding modelling.

Model parameter	Expression or correlation used in the present work	Ref.
Melting point [K]	1673	Schumann (1970)
Linear thermal expansion [%]	$\varepsilon_{th} = -3.101 \times 10^{-4} + 1.545 \times 10^{-5} \cdot T[^\circ\mathrm{C}] + 2.75 \cdot 10^{-9} \cdot T[^\circ\mathrm{C}]^2$	Gehr (1973)
Density [kg m^{-3}]	$\rho = 7900 \cdot \left(\frac{1}{(1+\varepsilon_{th})}\right)^3$	Schumann (1970) and Gehr (1973)
Specific heat [J kg^{-1} K^{-1}]	$C_p = 431 + 0.77 \cdot T[\mathrm{K}] + 8.72 \cdot 10^{-5} \cdot T[\mathrm{K}]^{-2}$	Banerjee et al. (2007)
Thermal conductivity [W m^{-1} K^{-1}]	$\lambda = 13.95 + 0.01163 \cdot T[^\circ\mathrm{C}]$	Többe (1975)
Young's modulus [GPa]	$E = 202.7 - 81.67 \times 10^{-3} \cdot T[^\circ\mathrm{C}]$	Többe (1975) and Pesl et al. (1987)
Poisson ratio	$\nu = 0.277 + 6 \times 10^{-5} \cdot T[^\circ\mathrm{C}]$.	Többe (1975) and Pesl et al. (1987)
Yield stress [MPa] at 0.2% strain	$\sigma_{Y,0.2\%} = \begin{cases} 555.5 - 0.25 \cdot T[^\circ\mathrm{C}] & \text{if } T < 600\ ^\circ\mathrm{C} \\ 405.5 - 0.775 \cdot (T[^\circ\mathrm{C}] - 600) & \text{if } 600\ ^\circ\mathrm{C} < T < 1000\ ^\circ\mathrm{C} \\ 345.5 - 0.25 \cdot T[^\circ\mathrm{C}] & \text{if } T > 1000\ ^\circ\mathrm{C} \end{cases}$	Többe (1975)
Ultimate tensile strength (UTS) [MPa]	$\sigma_{UTS} = \begin{cases} 700 - 0.3125 \cdot T[^\circ\mathrm{C}] & \text{if } T < 600^\circ\mathrm{C} \\ 512.5 - 0.96875 \cdot (T[^\circ\mathrm{C}] - 600) & \text{if } 600^\circ\mathrm{C} < T < 1000^\circ\mathrm{C} \\ 437.5 - 0.3125 \cdot T[^\circ\mathrm{C}] & \text{if } T > 1000^\circ\mathrm{C} \end{cases}$	Többe (1975)
Rupture strain [%]	$\varepsilon_{rupt} = 8 + 4.74 \times 10^{-3} \cdot (T[^\circ\mathrm{C}] - 500) + 6.2 \times 10^{-5} \cdot (T[^\circ\mathrm{C}] - 500)^2$	Többe (1975)

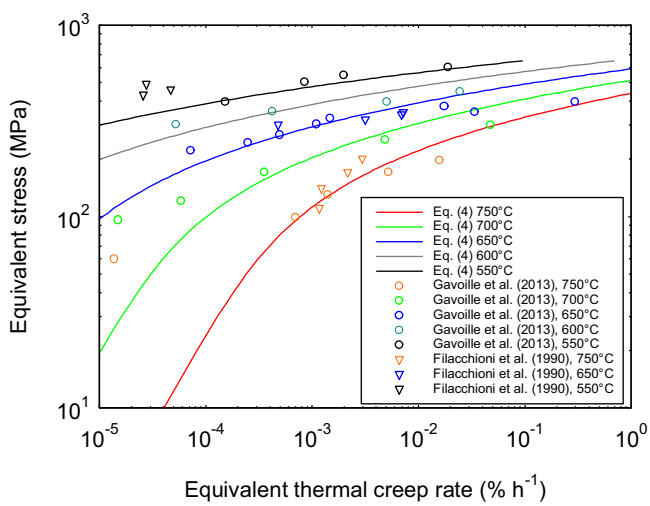

Fig. 3. Thermal creep correlation against creep experimental data (Filacchioni et al., 1990; Gavoille et al., 2013).

The "Specific AIM1" curve, represented in Eq. (2), refers to the best slot steel irradiated in the Phenix reactor, which should be closer to that proposed for ALFRED, i.e., similar to AIM1.

$$\frac{\Delta V}{V}[\%] = 1.3 \times 10^{-5} \exp\left[-2.5\left(\frac{T[^\circ\mathrm{C}] - 490}{100}\right)^2\right] \Phi^{3.9} \tag{2}$$

3.1.2. *Thermal and Irradiation creep*

As far as the thermal creep is concerned, the Nabarro–Herring description (Eq. (3)) suggested by Többe (1975) is adopted for the calculations:

$$\dot{\varepsilon}_\vartheta[\%\mathrm{h}^{-1}] = A \cdot \exp\left(\frac{-Q}{R \cdot T[\mathrm{K}]}\right) \sinh\left(\frac{V^* \cdot \sigma_{\mathrm{eq}}[\mathrm{MPa}]}{0.8075 \cdot R \cdot T[\mathrm{K}]}\right) \tag{3}$$

where R is the gas constant and $\dot{\varepsilon}_\vartheta$ the equivalent Von Mises thermal creep rate. Based on data from Gavoille et al. (2013), the constant A, the activation energy Q and the activation volume V^* have been set in order to obtain the best fit with the available AIM1 creep measurements. The formula presented in Eq. (4) is adopted for the calculations:

$$\dot{\varepsilon}_\vartheta[\%\mathrm{h}^{-1}] = 2.3 \times 10^{14} \cdot \exp\left(\frac{-84,600}{R \cdot T[\mathrm{K}]}\right) \sinh\left(\frac{34.54 \cdot \sigma_{\mathrm{eq}}[\mathrm{MPa}]}{0.8075 \cdot R \cdot T[\mathrm{K}]}\right) \tag{4}$$

In Fig. 3, the equivalent[2] thermal creep rate and the equivalent[2] stress (σ_{eq}) data found in Filacchioni et al. (1990) and Gavoille et al. (2013) are compared with the correlation implemented in TRANSURANUS.

The irradiation induced creep ($\dot{\varepsilon}_{\mathrm{irr}}$) is described by means of the following correlation (Többe, 1975):

$$\dot{\varepsilon}_{irr}[\%\mathrm{h}^{-1}] = 3.2 \times 10^{-24} \bar{E} \phi \sigma_{\mathrm{eq}}[\mathrm{MPa}] \tag{5}$$

where $\bar{E}$ is the mean neutron energy in MeV and ϕ is the neutron flux in n cm^{-2} s^{-1}.

3.1.3. *Thermal creep rupture time*

In order to evaluate the rupture time due to creep, a Cumulative Damage Function (CDF) based on the Larson-Miller Parameter (LMP) has been included in the TRANSURANUS code. Even if the adoption of austenitic steels as cladding material ensures a better creep behaviour with respect to the use of ferritic-martensitic steels, the thermal creep cladding failure can be of concern under Fuel Cladding Mechanical Interaction (FCMI) conditions (i.e., closed gap condition, see e.g., Waltar et al., 2011). In the present work, the cladding damage due to the chemical interaction between fission products and cladding (i.e., the FAE phenomenon) is not considered.

An evaluation of the time to rupture is usually made through the LMP, defined according to the following equation (Larson and Miller, 1952):

$$\mathrm{LMP} = T[\mathrm{K}][C + \log_{10}(t_r[\mathrm{h}])] \tag{6}$$

where C is a constant and t_r represents the time-to-rupture. The relative CDF can be defined in terms of rupture time as:

$$\mathrm{CDF} = \sum \frac{\Delta t}{t_r} \tag{7}$$

Although a CDF value smaller than one indicates that cladding does not fail because of thermal creep, a maximum value of 0.2–0.3 is generally considered acceptable (see Table 4).

Based on Filacchioni et al. (1990) the following correlations have been implemented:

$$\begin{cases} \mathrm{LMP} = T[\mathrm{K}](17.125 + \log_{10} t_r[\mathrm{h}]) \\ \mathrm{LMP} = \dfrac{2060 - \sigma_{\mathrm{eq}}[\mathrm{MPa}]}{0.095} \end{cases} \tag{8}$$

In Fig. 4, the comparison between the data available from Filacchioni et al. (1990) and the above correlations implemented in the code are reported.

[2] The Von Mises criterion of equivalence is applied for both the thermal creep rate and the stress in this paper.

Table 7
Correlations adopted in the lead coolant modelling (OECD/NEA Handbook, 2007).

Model parameter	Expression or correlation used in the present work
Melting point [K]	600.6
Boiling point [K]	2016
Density [kg m^{-3}]	$\rho = 11,367 - 1.1944 \cdot T\,[\mathrm{K}]$
Specific heat [J kg^{-1} K^{-1}]	$C_p = 175.1 - 4.961 \times 10^{-2} \cdot T[\mathrm{K}] + 1.985 \times 10^{-5} \cdot T[\mathrm{K}]^2 + -2.099 \times 10^{-9} \cdot T[\mathrm{K}]^3 - 1.524 \times 10^{6} \cdot T[\mathrm{K}]^{-2}$
Thermal conductivity [W m^{-1} K^{-1}]	$\lambda = 9.2 + 0.011 \cdot T[\mathrm{K}]$
Dynamic viscosity [Pa s]	$\eta = 4.55 \times 10^{-4} \cdot \exp\left(\frac{1069}{T[\mathrm{K}]}\right)$

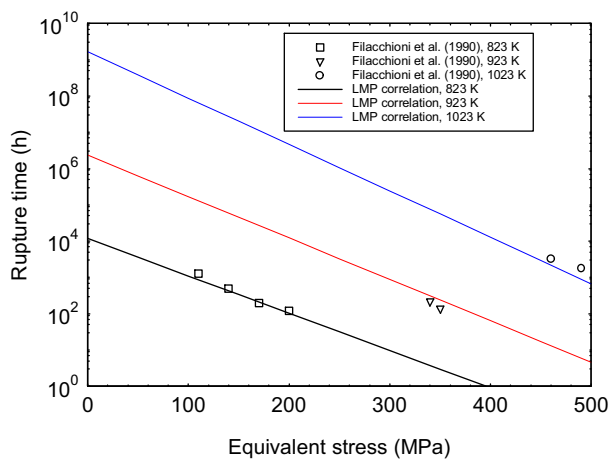

Fig. 4. LMP/rupture time correlation against the experimental data of Filacchioni et al. (1990).

3.2. Coolant

As far as the coolant is concerned, the main physical properties for liquid lead are available in the TRANSURANUS code. In particular, the melting and the boiling point, the correlations for density, heat capacity, and thermal conductivity are mainly based on the OECD/NEA Handbook (2007), and they have been subsequently revised by Agosti et al. (2013) for the implementation (Table 7).

One of the critical parameters of the lead is the convective heat transfer coefficient. In literature, several correlations for the Nusselt number (Nu) have been proposed to be used in the lead environment as a function of the pin pitch (p) and the rod diameter (D). In this work, the correlation proposed by Ushakov et al. (1977) for triangular rod bundles lattice has been adopted as recommended by several authors (Pfrang and Struwe, 2007; Mikityuk, 2009). The expression as a function of the Peclet number (Pe) and the range of validity are shown in Eq. (9).

$$Nu = 7.55\frac{p}{D} - 20\left(\frac{p}{D}\right)^{-13} + \frac{3.67}{90}\left(\frac{p}{D}\right)^{-2} Pe^{(0.56+0.19^{(p/D)})}$$
$$1.2 \le \frac{p}{D} \le 2.0 \qquad (9)$$
$$1 < Pe < 4000$$

3.3. Thermal-hydraulics, power history and neutronics input data

In Fig. 5a, the axial discretization of the fuel pin in the TRANSURANUS code is presented. Each slice is analysed at the middle, and all the input quantities (e.g., the linear power rate and the neutron flux) are constant along the slice.

Two different coolant channels of the ALFRED reactor have been investigated, namely: (i) the Average Channel (AC) representative of the average core condition; and (ii) the Hot Channel (HC), describing the most severe conditions achieved in the core in terms of power history. The AC (Fig. 5b) is defined as the triangular channel located in a generic sub-assembly and is characterized by the reactor average linear power, constant along the 5 irradiation years (1825 EFPDs). The HC (Fig. 5c) is located in the more enriched fuel assembly closer to the core centre.

Table 8
Main parameters of AC and HC modelling (Petrovich et al., 2013).

	AC	HC
Pin power [kW]	12.9	17.7
Lead mass flow rate [kg s^{-1}]	1.14	1.14
Burn-up [at.%]	7	9.5
Axial peak factor (Beginning of Cycle – BoC)	1.16	1.20
Axial peak factor (End of Cycle – EoC)	1.13	1.13
Total flux [n cm^{-2} s^{-1}]	1.53×10^{15}	1.6×10^{15}
Fast flux (>100 keV), [n cm^{-2} s^{-1}]	0.47×10^{15}	0.51×10^{15}
Fast flux (>10 keV), [n cm^{-2} s^{-1}]	0.93×10^{15}	1×10^{15}

In Table 8, the main parameters of the AC and HC modelling are presented. Fig. 6a shows the average linear power history for both AC and HC. The latter channel is characterized by the highest linear power, which decreases from the beginning of life (BoL) to the end of life (EoL) during the 5 yearly cycles. A realistic axial power profile is also provided to the code with a linear interpolation between the Beginning of Cycle (BoC) and End of Cycle (EoC) state (Fig. 6b).

Neutronics analysis of the ALFRED pin has been carried out by means of the SERPENT code (SERPENT, 2011), which is able to calculate the one-group neutron cross-sections and fast fluence to be provided to TRANSURANUS as input (Aufiero, 2013). In particular, the fast fraction of the flux is crucial for the determination of the radiation damage on the materials (e.g., related to swelling and irradiation creep). This value is also affected by large discrepancies in the literature, namely: (i) the threshold above which neutrons are considered fast enough to produce damage; and (ii) the "conversion factor" between fluence and displacement per atoms which is usually adopted in the correlations. These uncertainties will be taken into account in the sensitivity analysis (see Section 5).

4. Fuel pin performance results

In this section, TRANSURANUS results of the reference case are shown with a comparison between the average and the hot channel. In this analysis, the models and the parameters with the high degree of confidence and reliability with respect to the experimental data have been chosen, in order to give the "best estimate" evaluation of the fuel and cladding performance for the ALFRED reactor.

In the next section, a sensitivity analysis of the models and parameters affected by large uncertainties will be presented, with the aim to give a "conservative" evaluation of the pin behaviour through the adoption of the most severe combination of models.

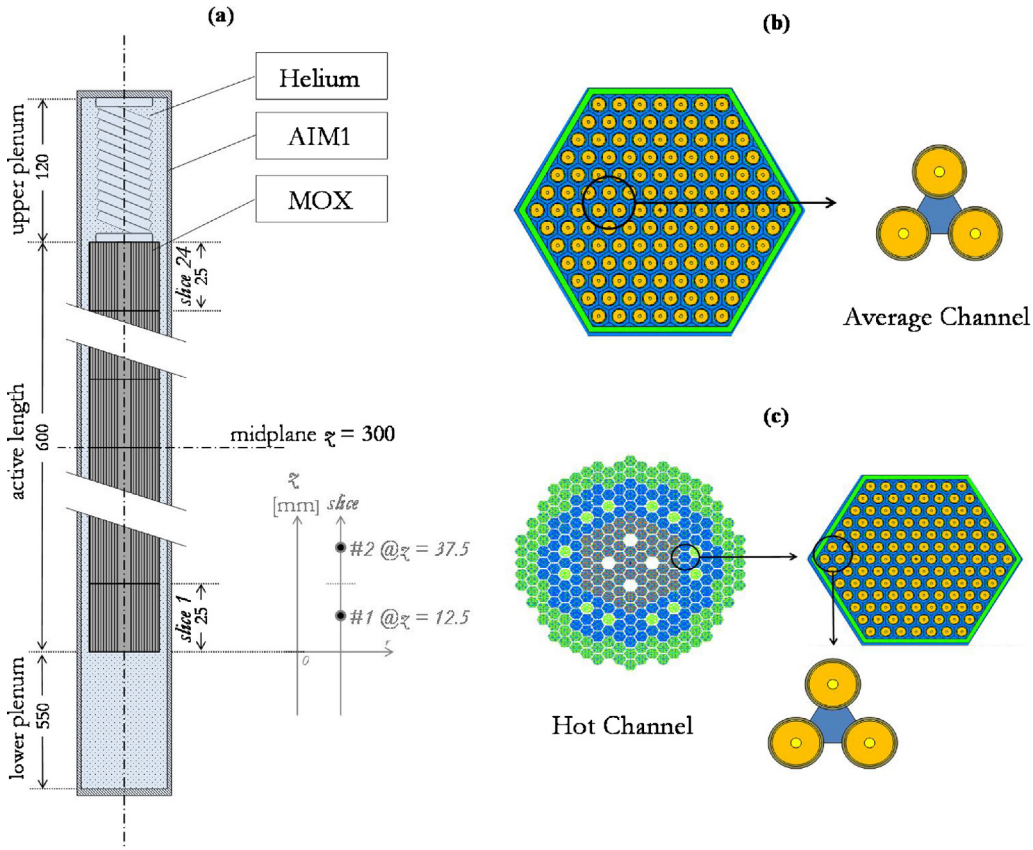

Fig. 5. Fuel pin modelling in the TRANSURANUS code: (a) axial discretization, (b) average channel, and (c) hot channel representation.

4.1. Fuel and cladding temperature

Fig. 7 shows the fuel temperature evolution during the irradiation for both the average and the hot channel at an axial elevation of 362.5 mm, along with the evolution of the gap conductance. For the average channel, the temperature is well below the limit (Table 4), reaching a maximum value of 1800 °C after the first irradiation cycle. Concerning the HC, the maximum temperature is higher, close to 2200 °C, due to the higher linear power, and occurs nearly at half of the first cycle (i.e., 1 at.% burn-up). This value is above the preliminary limit considered for the peak fuel temperature, established for granting a large margin to melting in case of an accident. The fuel temperature evolution is strongly influenced by the gap conductance. The maximum fuel temperature occurs at the minimum gap conductance, which occurs in the first part of the irradiation history. This peculiarity is due to the trade-off between the rate of the fission gas release and the reduction of the gap size. Afterwards, the conductance starts to sharply increase due to gap closing and, when the closure is complete, the inner and outer fuel temperatures settle to an almost constant level (the increase of gap conductance is counterbalanced by the fuel thermal conductivity degradation).

As far as the cladding and the coolant temperatures are concerned, the maximum temperatures are reached at the beginning

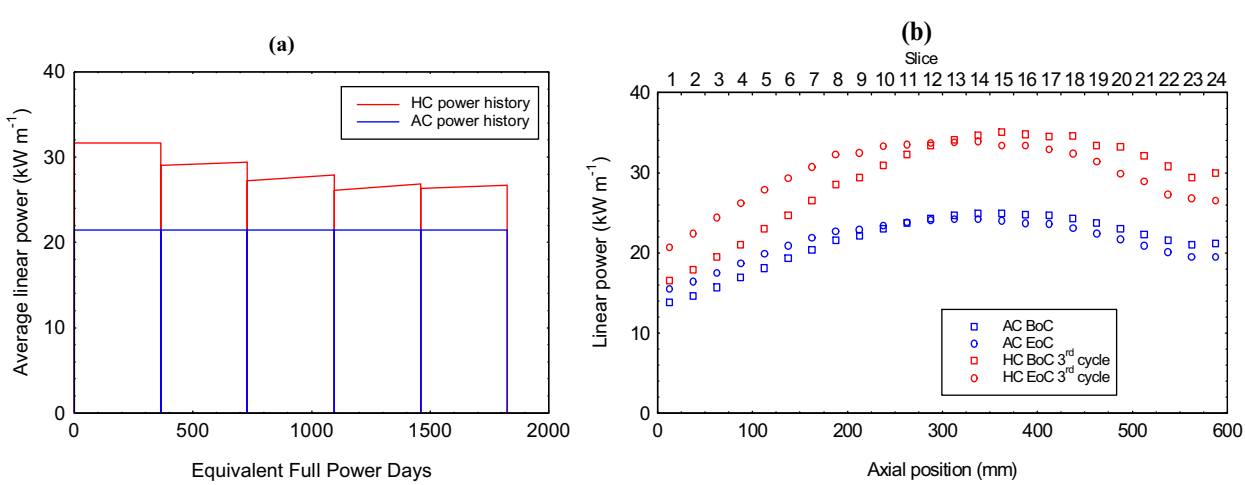

Fig. 6. (a) Average linear power history, and (b) the axial power profile for AC and HC at the beginning (BoC) and end (EoC) of the third cycle (Mattioli, 2012).

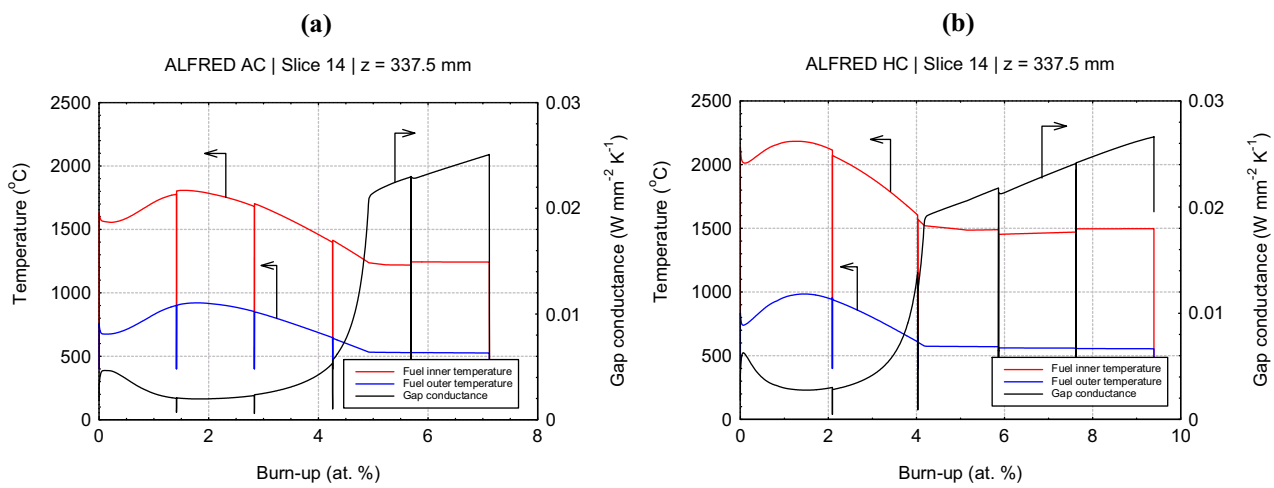

Fig. 7. Inner and outer fuel temperature, and gap conductance evolution versus burn-up for (a) AC and (b) HC reference case.

of the irradiation, at the end of the active length (Fig. 8). In addition, the relevant limit on the maximum external cladding temperature, proposed in order to reduce lead corrosion, is basically fulfilled in both the average and the hot channel, remaining below 550 °C during all the five batches.

4.2. Fission gas release

The Fission Gas Release (FGR) fraction along with the pin internal pressures (P) are shown in Fig. 9. As already mentioned, the higher linear power in the HC induces a higher maximum fuel temperature and, consequently, a higher FGR and pin pressure. For the average channel, the FGR reaches almost 60% at 2.5 at.% burn-up, whereas in the hot channel the FGR is 70% at 2 at.% burn-up. Due to fuel temperature decrease, the FGR decreases in the second part of the irradiation history, because the additional gas produced is retained in the fuel, rather than being released in the free volume. The internal pressure remains below the preliminary limit of 5 MPa (Table 4) both in the AC and the HC situation, suggesting a possible increase of the design value of the initial helium pressurization (at the moment fixed at 0.1 MPa), which will be discussed in Section 6.

4.3. Gap closing

The evolution of the gap size, the cladding inner radius and the fuel outer radius is described for the average and the hot channel in Fig. 10. The gap size dynamics is mostly driven by pellet deformation due to the progressive fuel swelling. In the average channel, the closure happens at a burn-up of 5 at.% (i.e., between the second and the third irradiation cycles). On the other hand, the hot channel, which is subjected to a higher linear heat rate, shows an anticipated gap closure at a burn-up of 4 at.% (i.e., at the end of the second cycle). Consequently, a stronger FCMI is observed in the hot channel since the gap is closed during most of the irradiation time, leading to the worsening of the cladding performance (i.e., higher stress as described in Section 4.4).

Since the gap dynamics is basically driven by the fuel thermal expansion and fuel swelling (in addition to clad creep down), the models of these two phenomena assume particular importance. Therefore, in the following section, a proper sensitivity will be performed focusing on the fuel swelling and the fuel conductivity models.

4.4. Stress and strain in the cladding

The radially averaged cladding equivalent stress at the axial peak power position, along with the contact pressure, is reported in Fig. 11. No issues regarding the cladding stress are observed as long as the gap is open. In this situation, the only contributions to the cladding stress state stem from the internal pressure and the thermal stresses, which are both relatively small. In particular, the

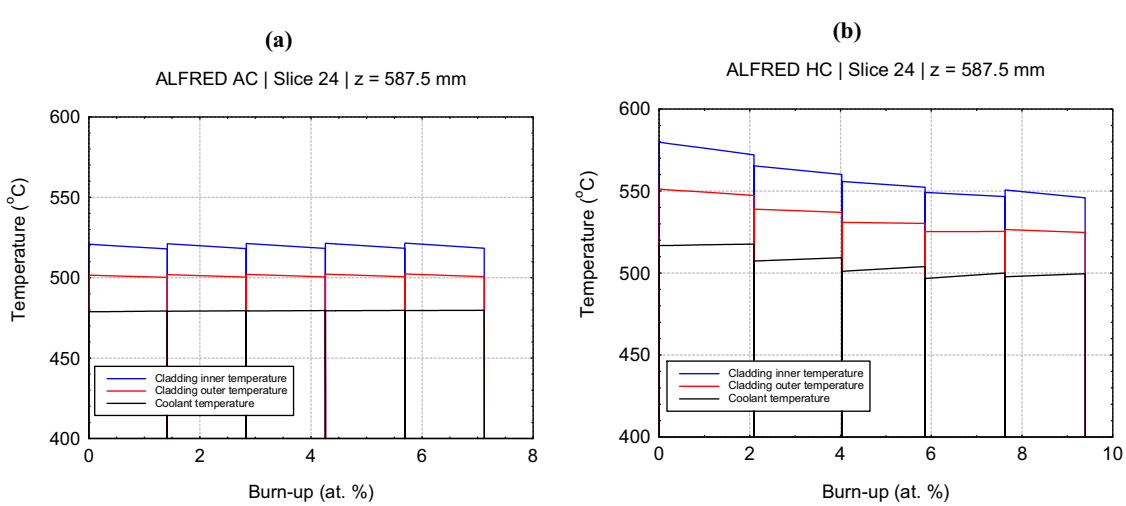

Fig. 8. Coolant and cladding temperature evolution for (a) AC and (b) HC reference case.

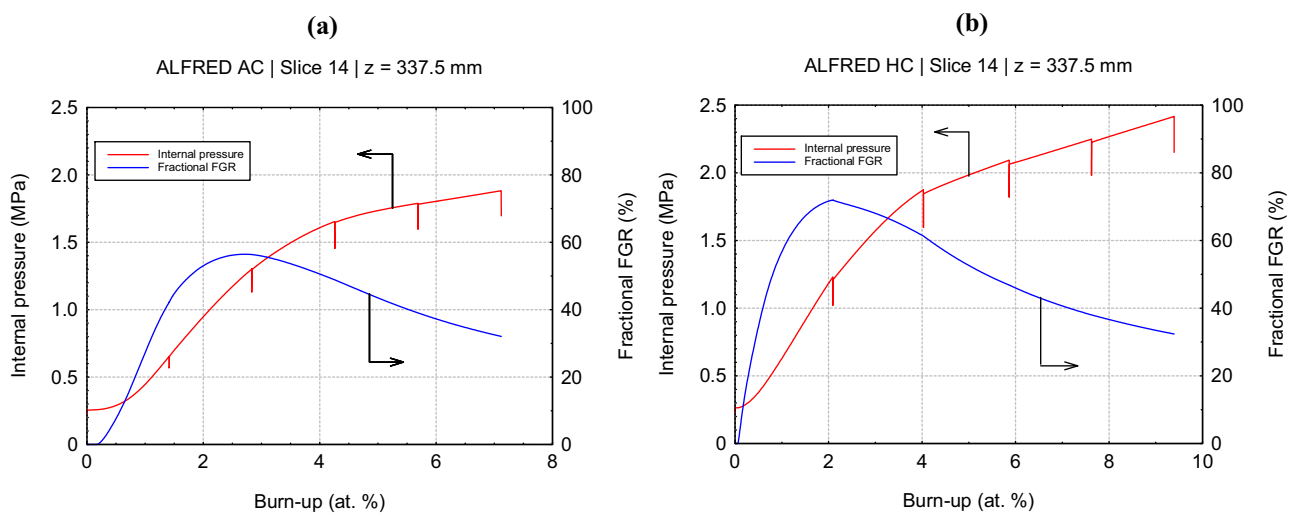

Fig. 9. Fission gas release (FGR) and internal pressure as a function of burn-up for (a) AC and (b) HC reference case.

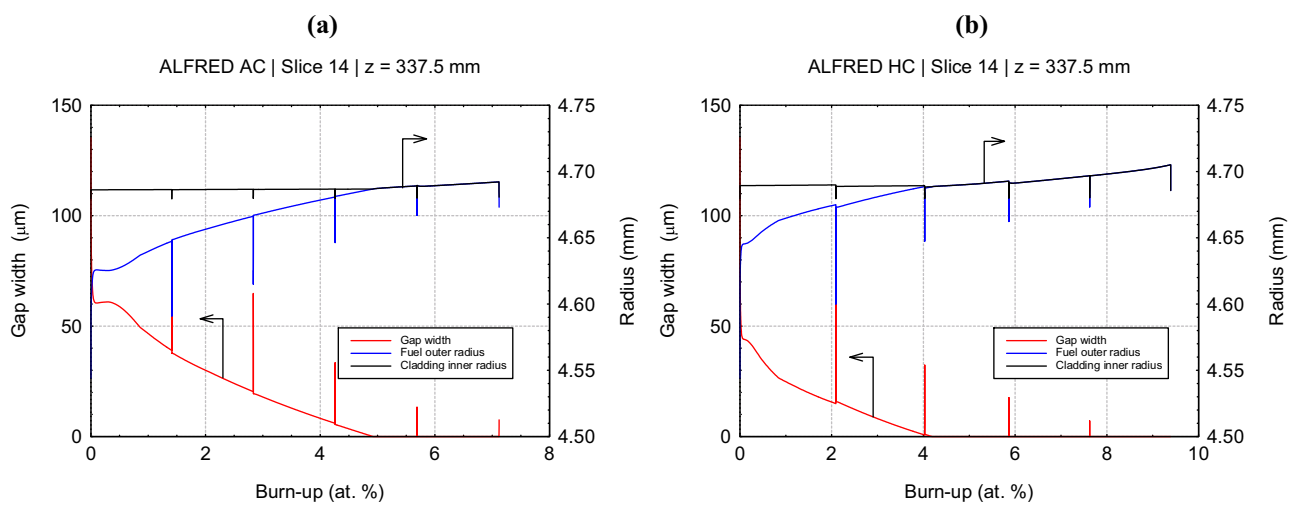

Fig. 10. Cladding inner and fuel outer radius, and gap width evolution as a function of burn-up for (a) AC and (b) HC reference case.

thermal stress is limited by the low temperature gradient across the cladding thickness (the cladding temperature drop is 25 °C for the average channel, and 35 °C for the hot channel). On the other hand, when the gap closes, the stress undergoes a sharp increase due to the FCMI caused by the progressive fuel swelling. As expected, due to the anticipated gap closure, the cladding stress in the HC is much higher compared to the AC. For the HC, this value is close to yielding, leading to a very low plastic strain at the EoL. The creep

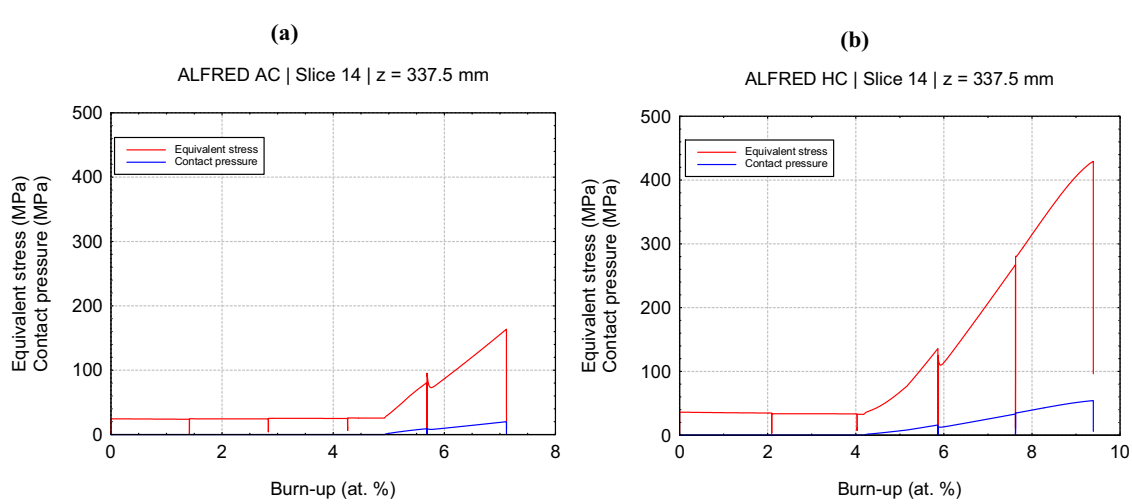

Fig. 11. Contact pressure between fuel and cladding along with the radially averaged equivalent stress in the cladding for (a) AC and (b) HC reference case.

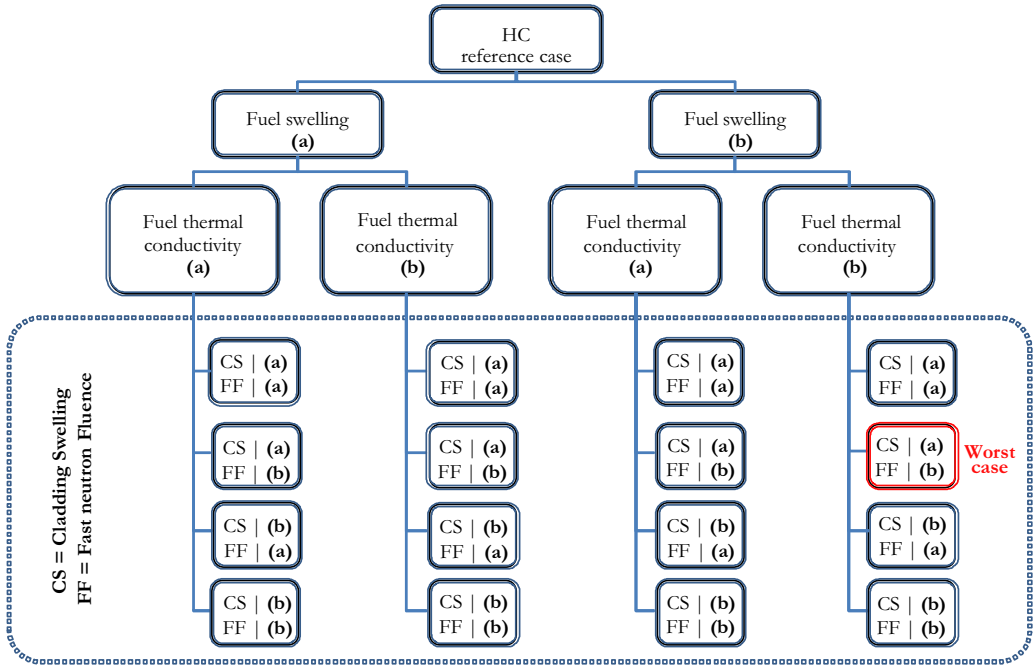

Fig. 12. Tree-graph of the sensitivity analysis, option (a) represents the models used in the reference analysis and option (b) the alternative candidates taken into account in the sensitivity analysis.

Table 9
TRANSURANUS results, at the EoL, for the average and hottest fuel pin of ALFRED reference case.

	AC	HC
FGR [%]	32	33
Average burn-up [at.%]	7.1	9.4
Maximum burn-up [at.%]	8.0	11.2
Maximum cladding swelling strain [%]	0.020	0.024
Maximum effective cladding thermal creep strain [%]	1.8×10^{-5}	0.086
Maximum effective cladding irradiation creep strain [%]	5.05×10^{-4}	8.84×10^{-4}
Maximum effective cladding plastic strain [%]	0	1.07×10^{-3}
Maximum fuel temperature [°C][a]	1810	2184
Maximum cladding outer temperature [°C]	497	551
Internal gas pressure [MPa]	1.70	2.41
CDF [-]	0.000	0.051

[a] This value refers to the maximum fuel temperature which occurs at about 1.5 at.% (i.e., not at EoL).

deformation is negligible (Table 9) and, consequently, stress relaxation is expected not occur, not even at the end of the irradiation time. In the average channel, the major contribution of the cladding creep strain is the irradiation induced phenomenon, whereas for the hot channel is the thermal effect. Both in the average and the hot channels, the strain design limits proposed in Table 4 are respected.

The presented cladding performance points out the high stress induced by FCMI for the hot channel and the respective thermal creep strain, suggesting a possible serious issue for the cladding integrity. Accordingly, the rupture time criterion based on the CDF described in Section 3.1.3 has been introduced in the analysis. The results show that the issue is not of concern for the ALFRED reactor, also in the hot channel case since the maximum CDF reaches 0.051 at the end of irradiation (the limit suggested by IAEA is 0.2/0.3 – see Table 4).

Table 10
Model options for the reference and the sensitivity analyses.[a]

Model	Option (a) selected in the reference analysis	Option (b) considered in the sensitivity analysis
Fuel swelling	1.2%/at.% with gap open, model of Preusser and Lassmann (1983)	2.0%/at.% with gap open, model of Pesl et al. (1987)
Fuel thermal conductivity	Model of Philipponneau (1992)	Model of Carbajo et al. (2001), higher deterioration effects due to burn-up
Cladding swelling	"Specific AIM1"	"Generalized Ti-15-15"
Fast neutron fraction	>100 keV	>10 keV

[a] For details, see TRANSURANUS Handbook (2013).

In Table 9, results for the average and the hot fuel pin of ALFRED are summarized. As a major outcome of the reference analysis, the AC turns out to be not affected by any issues in terms of fuel and cladding performance (all the limits shown in Table 4 are respected). On the other hand, the HC is characterized by high fuel inner temperature (i.e., above the preliminary limit) and large cladding stress.

5. Sensitivity analysis

In order to properly evaluate the impact of the uncertainties concerning some key models and input parameters used in the reference fuel performance (Section 4), a sensitivity analysis has been performed. The aim of this step is the definition of a "worst case" input for TRANSURANUS, based on the hot channel case. The results of the "worst case" scenario will be the starting point of the subsequent "optimization" phase (Section 6) aimed at improving the design of the ALFRED fuel pins.

As the main result of the reference analysis, the major weaknesses of the ALFRED fuel pin in the hottest reactor conditions are: (i) the maximum fuel temperature above the prescribed limit (Table 4), and (ii) the high stress level in the cladding due to FCMI.

Table 11
Model choice for the worst case.

Model	Worst case
Fuel swelling	Pesl et al. (1987)
Fuel thermal conductivity	Carbajo et al. (2001)
Cladding swelling	"Specific AIM1"
Fast neutron fraction	>10 keV

Table 12
TRANSURANUS results, at the EoL, for the average and hottest fuel pin of ALFRED worst case.

	Worst case AC	Worst case HC
FGR [%]	31	41
Average burn-up [at.%]	7.1	9.4
Maximum burn-up [at.%]	8.0	11.2
Maximum cladding swelling strain [%]	0.26	0.35
Maximum effective cladding thermal creep strain [%]	1.85×10^{-5}	0.135
Maximum effective cladding irradiation creep strain [%]	1.15×10^{-3}	1.96×10^{-3}
Maximum effective cladding plastic strain [%]	0	2.62×10^{-2}
Maximum fuel temperature [°C][a]	1816	2201
Maximum cladding outer temperature [°C]	497	551
Internal gas pressure [MPa]	1.86	2.97
CDF [-]	0.000	0.081

[a] At about 1.5 at.%

Accordingly, the models and the input parameters governing the fuel temperature evaluation and gap dynamics are more important for the sensitivity analysis. In particular, the fuel swelling, the fuel thermal conductivity, and the cladding swelling models have been selected for the sensitivity, along with the fast neutron fraction (which is coupled to the cladding swelling – see Eqs. (1) and (2)). Table 10 summarizes the models used in the reference analysis – Option (a) – and the alternative candidates taken into account in the sensitivity analysis – Option (b).

The figure of merit in the sensitivity analysis and worst case selection is the CDF. The latter has been selected since, besides taking into account the crucial FCMI, it is an integral quantity representing the fuel and cladding performance during the entire irradiation history.[3] Moreover, the CDF has turned out to be the most sensitive parameter, among other possible candidates, as "worst case" figure of merit. A tree-graph has been built (Fig. 12) in order to assess and evaluate the "worst case" between all the possible combinations. Through the TRANSURANUS simulations, the case characterized by the maximum CDF at EoL has been selected as the "worst case". The three levels of the tree represent the models involved in the analysis. A particular attention is due to the last level, which consists in the combination of cladding swelling model and the fast neutron fluence. In Table 11, the models defining the worst case scenario are reported.

5.1. Comparison between the reference and the worst case

It is useful to compare some important outputs between the worst case defined in this section and the HC reference case presented in Section 4. For the sake of brevity, only the temperature levels in the fuel, the stresses in the cladding, and the permanent strain components are shown.

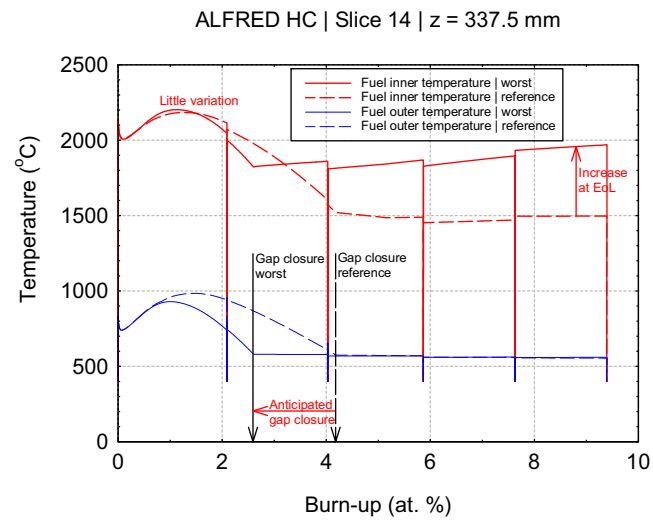

Fig. 13. Comparison between ALFRED HC reference case and worst case: fuel temperature evolution.

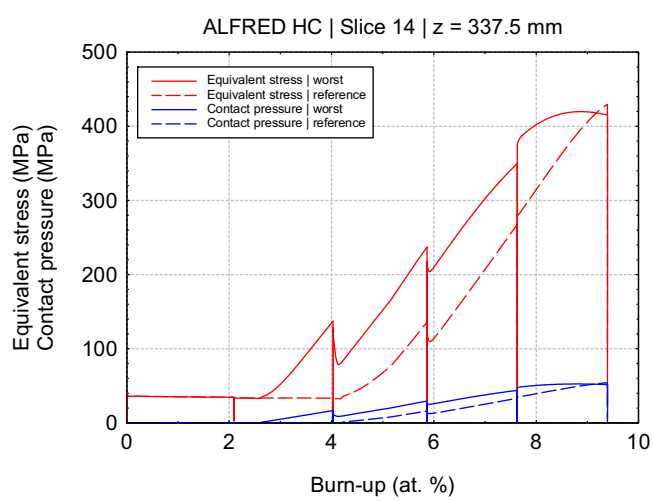

Fig. 14. Comparison between ALFRED HC reference case and worst case: radially averaged equivalent stress in the cladding.

As far as the fuel temperature is concerned (Fig. 13), the maximum value is almost the same for both the reference and the worst cases. Therefore, an optimization of the fuel pin may be required to allow increasing the safety margin against melting. In addition, although the temperature profiles of the worst case are slightly lower compared to the reference simulation in the first and second cycles (due to the anticipated gap closure), the trend is inverted in the last three cycles with a significant increase of the fuel inner temperature in the worst case.

The higher contact pressure is responsible for the higher stress in the worst case (Fig. 14), with a significant relaxation in the last period of irradiation due to the relevant swelling and thermal creep strains (Fig. 15).

In Table 12, results for the worst case scenario of the ALFRED fuel pin are summarized. The results of the sensitivity analysis indicate that the inner fuel temperature level still remains above the design limit in the HC worst case. In addition, possible issues may arise from the cladding stress and the thermal creep strain, whose values

[3] The maximum fuel temperature has not been considered as figure of merit since it represents the fuel behaviour at a particular time.

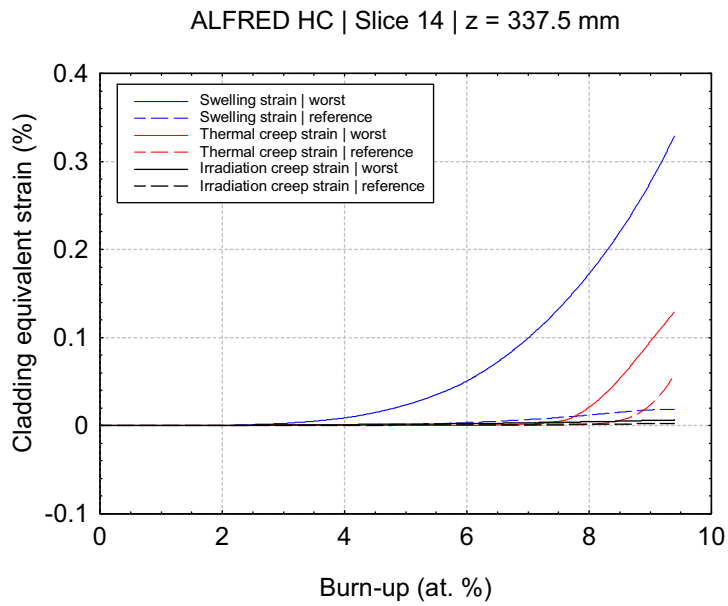

Fig. 15. Comparison between ALFRED HC reference case and worst case: permanent strain components.

Table 13
Design parameters.

Design parameter	Symbol	Range of variation	Unit
Initial gap width	g	{150; 175}	[μm]
Initial helium pressurization	p_{int}	{0.1; 0.3; 0.5}	[MPa]
Upper plenum height	h_{up}	{120; 180; 240}	[mm]

are more significant if the most conservative correlations are used in the TRANSURANUS code. On the other hand, encouraging results are found for the AC since no fuel and cladding performance issues are pointed out by the TRANSURANUS analysis, even in the worst case scenario.

6. Optimization

As last phase of this work, preliminary design optimizations are suggested, based on the results of the TRANSURANUS simulations, aimed at improving safety features of the ALFRED reactor. The TRANSURANUS integral performance code is particularly suited for this purpose since it is very difficult to predict a priori the influence of a slight change in design parameters, due to the large number of phenomena involved.

The results of the reference and worst case for ALFRED identify the high fuel temperature and the large stress in the cladding as the main issues regarding the fuel pin performance in the hottest condition of reactor. The purpose of the optimization phase described in this section is to reduce the impact of these drawbacks.

Keeping the current thermal-hydraulic and neutronic design, only minor changes are applied to those design parameters considered tuneable and suitable to improve the *safety-by-design* features of the reactor. The three parameters considered are: (1) the initial gap width, which can reduce the FCMI and consequently the cladding stress; (2) the initial internal helium pressure; (3) the upper plenum height. The two last parameters can improve the gap conductance and therefore can reduce the fuel temperature.

Several configurations of the fuel pin design can be defined assuming different values of the three tuneable parameters [g, p_{int}, h_{up}] (Table 13). In order to evaluate the impact of these configurations on the safety, five normalized figures of merit are defined (Table 14), starting from the design limits proposed in Table 4

Table 14
Figures of merit.

Normalized quantity	Symbol	Definition	Limit assumed
Fuel temperature	ϑ	T/T_{lim}	2273 K (2000 °C)
Internal pressure	π	P/P_{lim}	5 MPa
Thermal creep effective strain in the cladding	τ	$\varepsilon_{\vartheta}/\varepsilon_{\vartheta,lim}$	0.2%
CDF in the cladding	κ	CDF/CDF_{lim}	0.20
Plastic effective strain in the cladding	ε	$\varepsilon_p/\varepsilon_{p,lim}$	0.5%

(indicated with the subscript "lim" in Table 14) and involving the fuel temperature, the internal pin pressure, the thermal equivalent creep strain in the cladding, the CDF, and the plastic strain (ε_p) in the cladding [θ, π, τ, κ, ε].

The results are shown by means of a Kiviat diagram (or radar chart), which allows representing the five-dimensional space of the normalized quantities of interest. For the sake of clarity, in Fig. 16, only six out of eighteen possible configurations are represented. The evaluation of the impact in the fuel pin design modification has been studied on the worst case scenario for conservative purposes.

The effects of the slight change of fuel pin design on the safety performance are clearly stated. The higher internal

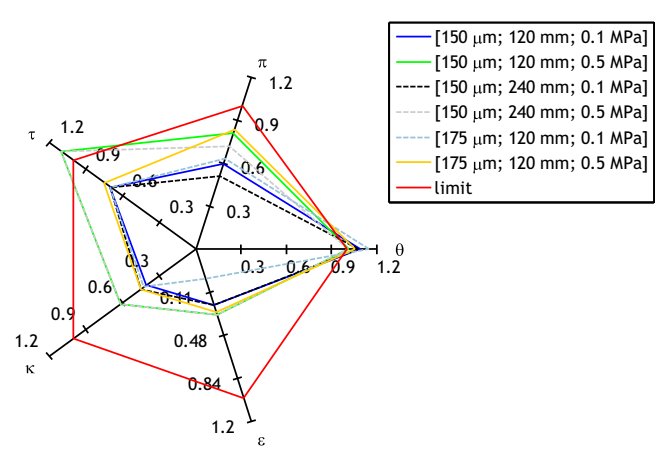

Fig. 16. Kiviat diagram of the most relevant fuel pin design configuration.

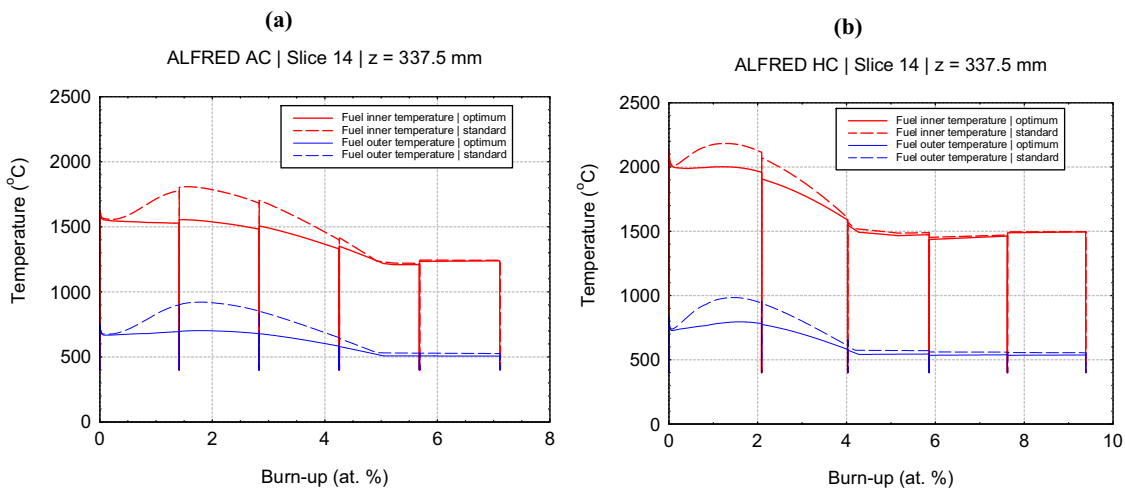

Fig. 17. Inner and outer fuel temperature evolution versus burn-up: comparison between the reference and the optimum case for (a) AC and (b) HC reference case.

Table 15
Comparison between the reference and the optimum case.

	AC		HC	
	Reference	Optimum	Reference	Optimum
FGR [%]	32	18	33	26
Maximum cladding swelling strain [%]	0.020	0.020	0.024	0.024
Maximum effective cladding thermal creep strain [%]	1.8×10^{-5}	1.8×10^{-5}	0.086	0.15
Maximum effective cladding irradiation creep strain [%]	5.05×10^{-4}	4.71×10^{-4}	8.84×10^{-4}	7.9×10^{-3}
Maximum effective cladding plastic strain [%]	0	0	1.07×10^{-3}	5.54×10^{-2}
Maximum fuel temperature [°C]	1810	1620	2184	1994
Internal gas pressure [MPa]	1.70	2.32	2.41	3.15
CDF	0.000	0.000	0.051	0.085

pre-pressurization value leads to an increase of the EoL pressure and, therefore, to an increase of both the thermal creep strain and CDF. As a major outcome of this "optimum" configuration, an effective decrease in the fuel temperature is predicted (Fig. 16), with benefit in terms of margin against melting in case of accident. The increase in the gap size seems to not bring a significant benefit. On the contrary, it leads to a general worsening of the performance. Finally, the increase in the upper plenum height has the only remarkable effect of decreasing the inner pressure. On the other hand, it is worthwhile to remind that this change has an impact on the natural circulation capabilities of the reactor, introducing additional pressure losses.

Given the optimization analysis, it is clear that the fuel temperature issue can be solved through the increase of the initial helium pressurization. Conversely, the stress in the cladding remains at high level after the optimization. Therefore, the increment of the initial internal pressure of the fuel pin from 0.1 MPa up to 0.5 MPa has been applied to the AC and HC reference case with the major outcome of limiting the fuel temperature below 2000 °C (Fig. 17). As expected, an increase of thermal creep strain and internal pressure is noticed, as shown in Table 15. Nevertheless, the indicative design limits proposed in Section 2.1 (see Table 4) are always respected.

Finally, in order to hold over the conservative approach adopted in this work, the optimized configuration (i.e., with the increase of the initial pressure) has been applied also to the HC worst case. Similarly to the reference case, in the optimized worst case the fuel temperature is reduced below the design limit proposed in Table 4. On the other hand, even if four out of five limits are respected, the cladding thermal creep strain is slightly above the required limit, reaching a total effective value of 0.22% in the optimized HC worst case (the limit is fixed at 0.2%), compared to 0.15% in the optimized reference case for the HC (Table 15). It is worthwhile to remind that, in case of thermal creep, the more conservative limit has been taken into account and the value reached in the optimized worst case simulation is very far from the other proposed limit (i.e., 1% thermal creep strain). In conclusion, also the optimization of the worst case can be considered satisfactory due to the large decrease of the maximum fuel temperature and the acceptable values of the other relevant figures of merit.

7. Conclusions

In this paper, the TRANSURANUS fuel performance code has been employed in the pin design analysis and optimization for the ALFRED reactor. Development efforts have been dedicated to the extension of the TRANSURANUS code for analysing LFRs, with reference to the materials adopted in the ALFRED design. In this work, the material properties of Ti-15-15 cladding have been implemented focusing on thermal creep and swelling behaviour.

The fuel and cladding performance concerning the average and the hottest reactor conditions has been investigated in the reference analysis (according to a "best estimate" approach) in the light of indicative and preliminary design limits. As main result of the reference analysis, the average channel exhibits a good performance and does not present critical issues, such as the maximum fuel and outer cladding temperatures well below the limits and the negligible cladding strain thanks to the low level of the corresponding stress. On the other hand, the major criticalities highlighted by the hot channel analysis are the high fuel inner temperature (i.e., above the design limit) and the large cladding stress due to FMCI. In order to assess the impact of the models and the parameters responsible for the fuel temperature and the gap dynamics, a sensitivity analysis has been performed considering the most severe conditions ("worst case" scenario) in terms of fuel swelling behaviour,

which turned out to be the main responsible for the performance worsening, fuel thermal conductivity, cladding swelling and fast neutron flux. The adoption of the conservative model combination confirms the good fuel and cladding performance for the average channel, whereas the fuel temperature and cladding stress issues are enhanced for the HC conditions.

Starting from the "worst case" scenario, the TRANSURANUS code has been employed in the optimization of the fuel pin design, aiming at improving the *safety-by-design* features of the ALFRED reactor. An increase of the initial helium pressurization of the fuel pin from 0.1 MPa to 0.5 MPa is advisable since a significant benefit in terms of fuel temperature reduction may be obtained without breaking the design limits both in average and hot channels. One the other hand, the cladding stress turned out to be difficult to reduce with minor changes of the design parameters. To this purpose, an optimization of the radial power peak factor of the reactor core may be suitable for overcoming the problem, given the satisfactory results obtained for the average channel.

The procedure adopted in this work revealed to be suitable for giving important feedback to the reactor designers in the conceptual design of ALFRED reactor. The capabilities of the TRANSURANUS integral performance code have been exploited to evaluate the synergy of the phenomena occurring in the fuel pin and their impact on the fuel pin design improvement, on the basis of operational power history simulations. Accidental simulations are beyond the scope of this work. Such analysis, along with additional investigation on the modelling uncertainties and model improvements (e.g., the dependence of the cladding swelling on the stress and the coupling with the creep phenomenon; the chemical fuel–cladding interaction; the JOG (Joint Oxide Gain) formation; the caesium migration; and, in general, the FCMI modelling), will be the object of future works.

Acknowledgments

The authors acknowledge the European Commission for funding the LEADER Project in the 7th Framework Programme. Acknowledgment is also due to all the colleagues of the participant organizations for their contributions in many different topics, in particular to Dr. Alessandro Alemberti and Dr. Luigi Mansani (Ansaldo Nucleare, Italy) for their valuable support and fruitful criticism. The authors wish to thank Dr. Giacomo Grasso and Dr. Carlo Petrovich (ENEA, Italy) for critical discussion and technical information, as well as Manuele Aufiero (Politecnico di Milano) for the neutronic analysis of the ALFRED reactor.

References

Agosti, F., Botazzoli, P., Di Marcello, V., Luzzi, L., Pastore, G., 2011. Fuel rod performance analysis for the Italian LBE-XADS: a comparison of two different cladding materials. In: Technology and Components of Accelerator-driven Systems, OECD NEA No 6897, ISBN 978-92-64-11727-3.

Agosti, F., Botazzoli, P., Di Marcello, V., Pastore, G., Luzzi, L., 2013. Extension of the TRANSURANUS code to the analysis of cladding materials for liquid metal cooled fast reactors: A preliminary approach. Technical Report, CESNEF-IN-02-2013.

Aït Abderrahim, H., Baeten, P., De Bruyn, D., Fernandez, R., 2012. MYRRHA – a multipurpose fast spectrum research reactor. Energ. Convers. Manage. 63, 4–10.

Alemberti, A., Carlsson, J., Malambu, E., Orden, A., Cinotti, L., Struwe, D., Agostini, P., Monti, S., 2010. From ELSY to LEADER – European LFR activities. In: Transactions of the American Nuclear Society, European Nuclear Conference 2010, Barcelona, Spain, May 30–June 2, 2010.

Alemberti, A., Carlsson, J., Malambu, E., Orden, A., Struwe, D., Agostini, P., Monti, S., 2011. European lead fast reactor – ELSY. Nucl. Eng. Des. 241, 3470–3480.

Alemberti, A., Frogheri, M., Mansani, L., 2013. The Lead Fast Reactor: Demonstrator (ALFRED) and ELFR Design. In: Proceedings of the IAEA International Conference on Fast Reactors and Related Fuel Cycles: Safe Technologies and Sustainable Scenarios (FR13), Paris, France, March 3–4, 2013.

Aufiero, M., 2013. ALFRED fuel pin neutronics characterization (private communication).

Banerjee, A., Raju, S., Divakar, R., Mohandas, E., 2007. High temperature heat capacity of alloy D9 using drop calorimetry based enthalpy increment measurements. Int. J. Thermophys. 28, 97–108.

Bergmann, H.J., Dietz, W., Ehrlich, K., Mühling, G., Schirra, M., 2003. Entwicklung des Werkstoffs X10CrNiMoTiB 15 15 als Strukturmaterial für Brennelemente. Technischer Bericht, FZKA 6864.

Bouineau, V., Di Marcello, V., Lainet, M., Van Uffelen, P., Walker, C., Chauvin, N., Pelletier, M., 2013. Assessment of SFR fuel pin performance codes under advanced fuel for minor actinide transmutation. In: Proceedings of the International Nuclear Fuel Cycle Conference GLOBAL 2013, Salt Lake City, UT, USA, September 29–October 3, 2013.

Cacuci, D.G., 2010. Lead-Cooled Fast Reactor (LFR) Design: Safety, Neutronics, Thermal Hydraulics, Structural Mechanics, Fuel, Core, and Plant Design. Handbook of Nuclear Engineering, vol. 4. Springer, Boston (chapter 23).

Carbajo, J.J., Yoder, G.L., Popov, S.G., Ivanov, V.K., 2001. A review of the thermophysical properties of MOX and UO2 fuels. J. Nucl. Mater. 299, 181–198.

Cheon, J.S., Lee, C.B., Lee, B.O., Raison, J.P., Mizuno, T., Delage, F., Carmack, J., 2009. Sodium fast reactor evolution: core materials. J. Nucl. Mater. 392, 324–330.

Di Marcello, V., Schubert, A., van de Laar, J., Van Uffelen, P., 2012. Extension of the TRANSURANUS plutonium redistribution model for fast reactor performance analysis. Nucl. Eng. Des. 248, 149–155.

Di Marcello, V., Botazzoli, P., Schubert, A., Van Uffelen, P., 2013. Improvements of the TRANSURANUS code for FBR fuel performance analysis. IAEA TECDOC 1689., pp. 137–149.

Di Marcello, V., Rondinella, V., Schubert, A., van de Laar, J., Van Uffelen, P., 2014. Modelling actinide redistribution in mixed oxide fuel for sodium fast reactors. Prog. Nucl. Energy 72, 83–90.

Dubuisson, P., 2013. Core structural materials – feedback experience from Phénix. IAEA TECDOC 1689, pp. 235–247.

Filacchioni, G., De Angelis, U., Ferrara, D., Pilloni, L., 1990. Mechanical and structural behaviour of the second double stabilized stainless steels generation. In: International Conference on Fast Reactor Core and Fuel Structural Behaviour, London, UK, June 4–6, 1990.

Frost, B.R.T., 1994. Mixed oxide fuel pin performance. Nuclear Materials, Materials Science and Technology Series, vol. 10B. VCH Verlagsgesellschaft GmbH/VCH Publishers, Inc (chapter 11).

García Ferré, F., Ormellese, M., Di Fonzo, F., Beghi, M.G., 2013. Advanced Al_2O_3 coatings for high temperature operation of steels in heavy liquid metals: a preliminary study. Corros. Sci. 77, 375–378.

Gavoille, P., Courcelle, A., Seran, J.L., Averty, X., Bourdiliau, B., Provitina, O., Garat, V., Verwaerde, D., 2013. Mechanical properties of cladding and wrapper materials for the ASTRID Fast-Reactor Project. In: Proceedings of the IAEA International Conference on Fast Reactors and Related Fuel Cycles: Safe Technologies and Sustainable Scenarios (FR13), Paris, France, March 3–4, 2013.

Gehr, H.L., 1973. Datensammlung zur Kernelementauslegung. Interatom – Technischer Bericht 73.30.

GIF, 2002. A Technology Roadmap for Generation IV Nuclear Energy Systems. Technical Report GIF-002-00.

Grasso, G., Petrovich, C., Mikityuk, K., Mattioli, D., Manni, F., Gugiu, D., 2013. Demonstrating the effectiveness of the European LFR concept: the ALFRED core design. In: Proceedings of the IAEA International Conference on Fast Reactors and Related Fuel Cycles: Safe Technologies and Sustainable Scenarios (FR13), Paris, France, March 3–4, 2013.

Hübner, H., 2000. Das Bestrahlungsverhalten des austenitischen Stahls DIN 1.4970. Technischer Bericht, FZKA6372, http://www.leader-fp7.eu/ (accessed 11.11.13).

IAEA, 2012a. Liquid Metal Coolants for Fast Reactors Cooled By Sodium, Lead, and Lead-Bismuth Eutectic. IAEA Nuclear Energy Series No. NP-T-1.6.

IAEA, 2012b. Structural Materials for Liquid Metal Cooled Fast Reactor Fuel Assemblies – Operational Behaviour. IAEA Nuclear Energy Series No. NF-T-4.3.

Larson, F.R., Miller, J., 1952. A time-temperature relationship for rupture and creep stresses. Trans. ASME 74, 765–771.

Lassmann, K., 1987. The OXIRED model for redistribution of oxygen in nonstoichiometric uranium–plutonium oxides. J. Nucl. Mater. 150, 10–16.

Lassmann, K., 1992. TRANSURANUS: a fuel rod analysis code ready for use. J. Nucl. Mater. 188, 295–302.

Lassmann, K., Benk, H., 2000. Numerical algorithms for intragranular fission gas release. J. Nucl. Mater. 280, 127–135.

Lassmann, K., Hohlefeld, F., 1987. The revised URGAP model to describe the gap conductance between fuel and cladding. Nucl. Eng. Des. 103, 215–221.

Lassmann, K., O'Carroll, C., van de Laar, J., Walker, C.T., 1994. The radial distribution of plutonium in high burnup UO_2 fuels. J. Nucl. Mater. 208, 223–231.

Mattioli, D., 2012. TH analysis of LFR Fuel Assembly. In: 3rd LEADER International Workshop: Design and safety analysis of ALFRED, Bologna, Italy, September 6 2012.

Mikityuk, K., 2009. Heat transfer to liquid metal: review of data and correlations for tube bundles. Nucl. Eng. Des. 239, 680–687.

NEA, 2005. Fuels and Materials for Transmutation. OECD NEA Technical Report No. 5419., ISBN 92-64-01066-1.

OECD/NEA, 2007. Handbook on Lead-bismuth Eutectic Alloy and Lead Properties, Materials Compatibility, Thermal-hydraulics and Technologies 2007 Edition, OECD NEA No. 6195., ISBN 978-92-64-99002-9.

Pesl, R., Freund, D., Gärtner, H., Steine, H., 1987. SATURN-S, Ein Programmsystem zur Beschreibung des thermomechanischen Verhaltens von Kernreaktorbrennstäben unter Bestrahlung. Technischer Bericht, KFK 4272.

Petrovich, C., Mikityuk, K., Manni, F., Gugiu, D., Grasso, G., 2013. ALFRED core. Summary, synoptic tables, conclusions and recommendations. ENEA Technical Report UTFISSM-P9SZ-006.
Pfrang, W., Struwe, D., 2007. Assessment of Correlations for Heat Transfer to the Coolant for Heavy Liquid Metal Cooled Core Designs. FZKA 7352, Karlsruhe.
Philipponneau, Y., 1992. Thermal conductivity of $(U,Pu)O_{2-x}$ mixed oxide fuel. J. Nucl. Mater. 188, 194–197.
Preusser, T., Lassmann, K., 1983. Current status of the transient integral fuel element performance code URANUS. In: International Conference on Structural Mechanics in Reactor Technology (SMiRT), paper C 4/3, Chicago, USA, August 22–26, 1983.
Schubert, A., Van Uffelen, P., van de Laar, J., Walker, C.T., Haeck, W., 2008. Extension of the TRANSURANUS burn-up model. J. Nucl. Mater. 376, 1–10.
Schumann, U., 1970. MAPLIB, A program system for provision of material property data to computer programs. KFK 1253.
SERPENT, 2011. PSG2/Serpent Monte Carlo Reactor Physics Burnup Calculation Code. http://montecarlo.vtt.fi
Sobolev, V., Malambu, E., Aït Abderrahim, H., 2009. Design of a fuel element for a lead-cooled fast reactor. J. Nucl. Mater. 385, 392–399.
Többe, H., 1975. Das Brennstabrechenprogramm IAMBUS zur Auslegung von Schellbrüter – Brenn – stäben. Technischer Bericht, ITB 75.65.
TRANSURANUS Handbook, 2013. Copyright© 1975–2013. European Commission.
Ushakov, P.A., Zhukov, A.V., Matyukhin, N.M., 1977. Heat transfer to liquid metals in regular arrays of fuel elements. Translated from Teplofizika Vysokikh Temperatur, vol. 15, No. 5.
Van Uffelen, P., Schubert, A., van de Laar, J., Győri, C., Elenkov, D., Boneva, S., Georgieva, M., Georgiev, S., Hózer, Z., Märtens, D., Spykman, G., Hellwig, C., Nordstrøm, Á., Luzzi, L., Di Marcello, V., Ott, L., 2007. The verification of the TRANSURANUS fuel performance code – an overview. In: Proceedings of 7th International Conference on WWER Fuel Performance, Modelling and Experimental Support, Albena, Bulgaria, September 17–21, 2007.
Vettraino, F., Luzzi, L., September 2001. ADS-demo Fuel Rod Analysis Report. ENEA-DT-SBD.00033 Technical Report., pp. 1–93.
Waltar, A.E., Todd, D.R., Tsvetkon, P.V., 2011. Fast Spectrum Reactors. Springer, New York.
Weisenburger, A., Schroer, C., Jianu, A., Heinzel, A., Konys, J., Steinera, H., Müller, G., Fazio, C., Gessi, A., Babayan, S., Kobzova, A., Martinelli, L., Ginestar, K., Balbaud-Célerier, F., Martín-Muñoz, F.J., Soler Crespo, L., 2011. Long term corrosion on T91 and AISI1 316L steel in flowing lead alloy and corrosion protection barrier development: experiments and models. J. Nucl. Mater. 415 (3), 260–269.